A photonic crystal side-coupled waveguide based on a high-quality-factor resonator array

2012 Chinese Phys. B 21 034215

(http://iopscience.iop.org/1674-1056/21/3/034215)

A photonic crystal side-coupled waveguide based on a high-quality-factor resonator array*

Cui Nai-Di(崔乃迪)[a)b)], Liang Jing-Qiu(梁静秋)[a)],
Liang Zhong-Zhu(梁中翥)[a)], and Wang Wei-Biao(王维彪)[a)†]

[a)] *State Key Laboratory of Applied Optics, Changchun Institute of Optics, Fine Mechanics and Physics, Chinese Academy of Sciences, Changchun* 130033, *China*

[b)] *Graduate University of Chinese Academy of Sciences, Beijing* 100049, *China*

(Received 20 July 2011; revised manuscript received 25 October 2011)

Based on the present coupled mode theory of the photonic crystal resonator array in this paper, we propose a novel side-coupled waveguide to achieve highly efficient coupling of photonic crystal devices. It is found that the coupling efficiency is sensitive to the interval, the total number and the quality factor of the resonator. Considering the coupling efficiency and the coupling region, we select five resonators with an interval of six lattice periods. By optimizing the structure parameters of the waveguide and resonator, the quality factors of the resonator can be modulated and the coupling efficiency of the side-coupled waveguide reaches 95.47% in theory. Compared with other coupling methods, the side-coupled waveguide can realize efficient coupling with a compact structure, a high level of integration and a low degree of operational difficulties.

Keywords: side-coupled waveguide, photonic crystal, high-quality-factor cavity

PACS: 42.70.Qs, 42.79.Gn, 42.82.Et **DOI:** 10.1088/1674-1056/21/3/034215

1. Introduction

Photonic crystals (PCs) are promising structures for optoelectronic integration and all-optical devices owing to their unique features in controlling the flow of light.[1−4] So far, PCs have been exploited for realizing highly compact optoelectronic devices such as PC waveguides,[5−8] optical switches[9,10] and couplers.[11−14] Because of their ultra-compact structures, PCs are envisaged as the main candidates to implement future integrated photonic/optical circuits.

The issue of how to couple light to PC devices has attracted much attention because of its significant value in optoelectronic integration.[15−19] The key problem with efficient coupling is the small volume and coupling region of the PC devices.[15−17] Many traditional coupling methods have been proposed, such as geometry optics coupling (GOC) [18,19] and evanescent-wave coupling (EWC).[20,21] For the GOC method, the lightwaves are coupled to the PC devices from the end face by external optical elements, such as focusing lenses, gratings and fiber tapers. Insertion and scattering losses owing to the use of the external optical elements influence the coupling efficiency dramatically. The small coupling region also leads to a high degree of operational difficulty. The EWC method enlarges the coupling region through coupling the lightwaves on the top of the PC devices. In 2004, Barclay *et al.* reported that near-unity coupling efficiency could be gained using the EWC method.[20] The coupling part (fiber taper) and the PC devices are independent of each other, and the distance between the fiber taper and the PC waveguide is difficult to control accurately. Moreover, the independence of the coupling part and the PC devices leads to a complicated structure, and thus a low integration level. A new approach, supporting a compact structure, a low degree of operational difficulty and a high integration level, is therefore of significant value.

In this paper, we investigate the coupling mode theory of the resonator array and propose a novel efficient PC side-coupled waveguide (SCW) to couple the light from the light source to the PC devices efficiently. The SCW is composed of a PC waveguide and a coupling part that relies on a high-quality-factor (Q) PC resonator array. Lightwaves are coupled into the PC waveguide from the light source through the high-Q PC resonator array. Compared with GOC and

*Project supported by the National Natural Science Foundation of China (Grant No. 60877031).

†Corresponding author. E-mail: wangwbt@126.com

EWC methods, the coupling region of the SCW is enlarged by introducing the high-Q resonator array. Additionally, the coupling part and the waveguide are integrated in one substrate. Thus, the position parameters of the coupling part and waveguide are optimized and fixed, and the operational difficulty decreases. The integration of the coupling part and the PC waveguide also brings a more compact structure and a high integration level. Integrated with PC optoelectronic or all-optical devices, SCWs can also be utilized as the incident terminal of PC devices, which shows great universality and compatibility.

2. The coupling mode theory of high-Q resonator arrays

Figure 1 shows the coupling width of an SCW ($W_{\rm s}$) and the width of a PC waveguide (W). $W_{\rm s}$ is decided by the amount of resonators. By introducing the resonator array, we can increase the coupling width and consequently the coupling region ($S_{\rm s} = W_{\rm s} \times h$, where h is the thickness of the PC). Take the PC devices in the optical communication waveband for instance, the coupling width of the traditional coupling method is typically only several hundreds of nanometers. In contrast, the SCW can increase the coupling width up to tens of micrometers or even larger. The SCW with a large coupling region permits large-scale light sources and can output more power, which makes pre-focusing and collimation easier. Additionally, the SCW with a large coupling region reduces the difficulty of the coupling between the PC and the fiber taper.

The amplitude of the selecting wave is denoted by a. The resonant frequency and the Q factor due to the intrinsic loss of the resonators are denoted by ω_0 and Q_0, respectively. The amplitudes of the incoming or outgoing waves for the resonator of number n ($1 \leq n \leq l$) are denoted by S_n, S'_{-n}, S'_n, S_{-n}, A_n, and A_{-n}, respectively. The squared magnitude of the amplitude is equal to the energy in the mode.

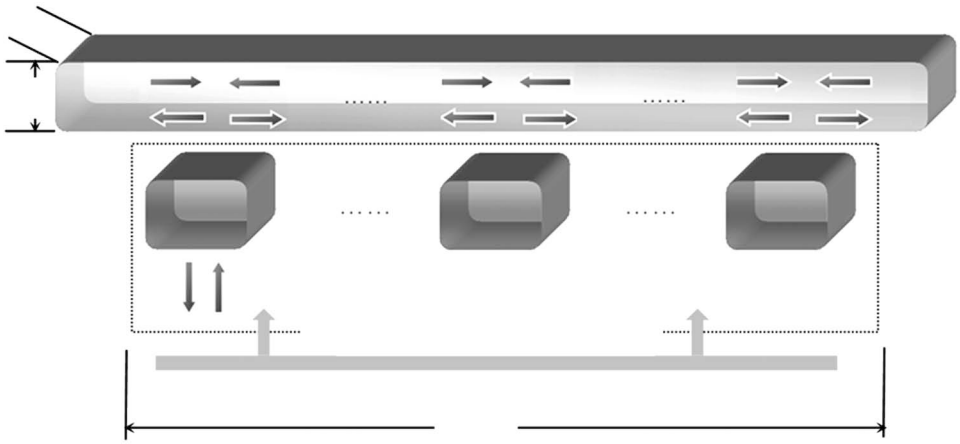

Fig. 1. A schematic of the SCW. A high-Q resonator array is placed on the side of the PC waveguide, and light is coupled into the PC waveguide through the high-Q resonator array.

According to coupling theory,[22–25] the time evolution of the resonator is described as follows:

$$\begin{aligned}\frac{{\rm d}a}{{\rm d}t} = &\left({\rm j}\omega_0 - \frac{\omega_0}{Q_0} - \frac{\omega_0}{2Q_{\rm b}} - \frac{\omega_0}{2Q_{\rm d}}\right)a \\ &+ {\rm e}^{{\rm j}\theta_{\rm b}}\sqrt{\frac{\omega_0}{2Q_{\rm b}}}S'_n + {\rm e}^{{\rm j}\theta_{\rm b}}\sqrt{\frac{\omega_0}{2Q_{\rm b}}}S_n \\ &+ {\rm e}^{{\rm j}\theta_{\rm d}}\sqrt{\frac{\omega_0}{2Q_{\rm d}}}A_n, \qquad (1)\end{aligned}$$

where $Q_{\rm b}$ and $Q_{\rm d}$ are the Q factors related to the rate of coupling into the waveguide and decay out of the resonators, respectively. $\theta_{\rm b}$ and $\theta_{\rm d}$ are the phases of the coupling coefficients between the resonators and the bus waveguide or incident wave, respectively.

According to power conservation and time-reversal symmetry, the relationship among the amplitudes of the incoming or outgoing waves can be expressed by

$$S'_{-n} = \frac{1}{2}A_n + S_n - {\rm e}^{-{\rm j}\theta_{\rm b}}\sqrt{\frac{\omega_0}{2Q_{\rm b}}}a, \qquad (2)$$

$$S_n = \frac{1}{2}A_n + S'_n - {\rm e}^{-{\rm j}\theta_{\rm b}}\sqrt{\frac{\omega_0}{2Q_{\rm b}}}a, \qquad (3)$$

$$S_{(n+1)} = S'_{-n}r, \quad S'_n = S^r_{-(n+1)}, \qquad (4)$$

where $r = \mathrm{e}^{-\mathrm{j}\beta d}$, β is the propagation constant in the bus waveguide, and d is the interval of the resonators. The coupling efficiency is defined as follows:

$$\eta = \frac{\left|S_{-1}^2\right| + \left|S_{-l}'^2\right|}{\left(\left|\sum_1^l A_n\right|\right)^2}. \tag{5}$$

In the coupling system, the electromagnetic wave is coupled from the side of the SCW. Consequently, $S_1 = 0$, $S_l' = 0$, and the amplitude of the selecting wave (a) has a $\mathrm{e}^{\mathrm{j}\omega t}$ time dependence. By solving Eqs. (2)–(4), S_n and S_n' are written as

$$\begin{aligned} S_n =& \frac{1}{2}(A_1 r^{(n-1)} + A_2 r^{(n-2)} + \cdots + A_{n-1} r) \\ & - \mathrm{e}^{-\mathrm{j}\theta_\mathrm{b}} \sqrt{\frac{\omega_0}{2Q_\mathrm{b}}} (r + r^2 + \cdots + r^{(n-1)}) a, \end{aligned} \tag{6}$$

$$\begin{aligned} S_n' =& \frac{1}{2}(A_{n+1} r + A_{n+2} r^2 + \cdots + A_l r^{(l-n)}) \\ & - \mathrm{e}^{-\mathrm{j}\theta_\mathrm{b}} \sqrt{\frac{\omega_0}{2Q_\mathrm{b}}} (r + r^2 + \cdots + r^{(l-n)}) a. \end{aligned} \tag{7}$$

By solving Eqs. (4), (6) and (7), the resulting expressions of S_{-1} and S_{-l}' are given by

$$\begin{aligned} S_{-1} =& S_{-l}' = \frac{1}{2}(A_1 r^{(l-1)} + A_2 r^{(l-2)} + \cdots + A_l) \\ & - \mathrm{e}^{-\mathrm{j}\theta_\mathrm{b}} \sqrt{\frac{\omega_0}{2Q_\mathrm{b}}} (r + r^2 + \cdots + r^{(l-1)} + 1) a. \end{aligned} \tag{8}$$

Inserting Eqs. (6) and (7) into Eq. (1), we obtain

$$\begin{aligned} Ha + \frac{\omega_0}{2Q_\mathrm{b}} Ia =& \frac{1}{2}(A_1 r^{n-1} + \cdots + A_{n-1} r \\ & + A_{n+1} r + \cdots + A_l r^{l-n}) \tau_\mathrm{b} \\ & + \tau_\mathrm{d} A_n. \end{aligned} \tag{9}$$

If we suppose that

$$H = \mathrm{j}\omega - \mathrm{j}\omega_0 + \frac{\omega_0}{Q_0} + \frac{\omega_0}{2Q_\mathrm{b}} + \frac{\omega_0}{2Q_\mathrm{d}},$$

$$I = r + r^2 + \cdots + r^{n-1} + r + r^2 + \cdots + r^{l-n},$$

A_n can be derived by solving Eq. (9). The coupling efficiency can be obtained by inserting Eq. (8) and A_n into Eq. (5). Herein, since the expressions of A_n and the coupling efficiency are extremely complicated, the detailed expression of the coupling efficiency will be given in the appendix.

Figure 2 shows the coupling efficiency as functions of $\beta d/\pi$ at the resonance frequency. It can be found that the coupling efficiency is sensitive to βd. The maximum coupling efficiency can be obtained when $\beta d = 2n\pi$ ($n = 0, 1, 2, \ldots$).

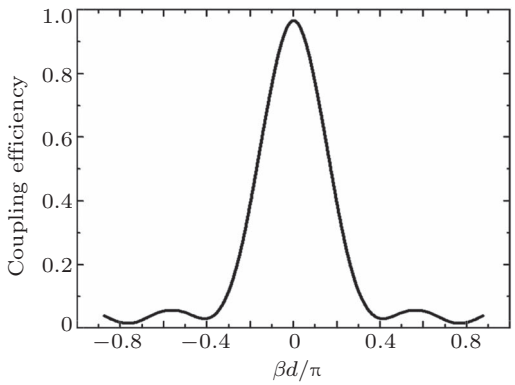

Fig. 2. The curve of the coupling efficiency as functions of $\beta d/\pi$ at the resonance frequency.

When the Gaussian wave is launched and $\beta d = 2n\pi$ ($n = 0, 1, 2, \ldots$), Eq. (8) can be written as

$$S_{-l}' = S_{-1} = \frac{1}{2} \sum_{-(l+1)/2}^{(l+1)/2} A_n - l\, \mathrm{e}^{-\mathrm{j}\theta_\mathrm{b}} \sqrt{\frac{\omega_0}{2Q_\mathrm{b}}} a. \tag{10}$$

From Eq. (9), the calculated result of A_n can be written as

$$A_n = \mathrm{e}^{-x^2} \frac{2H + (l-1)\dfrac{\omega_0}{Q_\mathrm{b}}}{(l-1)\,\mathrm{e}^{\mathrm{j}\theta_\mathrm{b}} \sqrt{\dfrac{\omega_0}{2Q_\mathrm{b}}} + 2\,\mathrm{e}^{\mathrm{j}\theta_\mathrm{d}} \sqrt{\dfrac{\omega_0}{2Q_\mathrm{d}}}} a, \tag{11}$$

where e^{-x^2} is the Gaussian factor. By inserting Eqs. (10) and (11) into Eq. (5), the coupling efficiency of the SCW excited by the Gaussian wave is given by

$$\eta = \left(\frac{S_{-1} S_{-l}}{\sum\limits_{-(l+1)/2}^{(l+1)/2} A(x)} \right)^2 = \left(1 - \frac{l}{\sum\limits_{-(l+1)/2}^{(l+1)/2} \mathrm{e}^{-x^2}} \times \frac{(l-1)\, Q_0 Q_\mathrm{d} + 2Q_0 \sqrt{Q_\mathrm{b} Q_\mathrm{d}}}{2Q_\mathrm{b} Q_\mathrm{d} + Q_0 Q_\mathrm{b} + l Q_0 Q_\mathrm{d}} \right)^2. \tag{12}$$

From Eq. (12), we can see that the coupling efficiency is sensitive to the following factors: the total number of the resonators (l), Q_0, Q_b and Q_d. Figure 3(a) gives the coupling efficiency as functions of Q_0 and the total number of resonators when Q_b and Q_d are, respectively, 10^4 and 10^2. It can be observed

that the coupling efficiency declines with the increasing total number of the resonators, and the coupling efficiency reaches the peak when there is only one resonator. However, the coupling region is decided by the amount of resonators, as shown in Fig. 1. Five resonators are selected for the coupling part of the device because when five resonators are introduced, the width of the SCW is about 15 μm, and the coupling efficiency can still reach 90% or higher. The coupling efficiency is also sensitive to Q_0. For appropriately-designed resonators and a large enough amount of surrounding photonic crystal material, the intrinsic loss of the cavity is attributed to the reflection loss at the interface between the interior and exterior of the cavity.[26−28] For the two-dimensional (2D) PC resonators, most of the intrinsic loss comes from the vertical loss of the lightwaves. One of the best approaches to this problem is the PC slab, in which the lightwaves are confined by total internal reflection at the interface between the substrate and air clad in a vertical direction. Therefore, by appropriately designing the structure of the resonators in the PC slab, the intrinsic loss can be controlled at a low level. In addition, Tada *et al.* proposed that the vertical loss of 2D PC devices can also be restrained by depositing Ag on the surface of the substrate and capping an Si substrate coated by Ag on the top.[29,30] The coupling efficiency as functions of Q_b and Q_d is shown in Fig. 3(b) for an SCW composed of five resonators and $Q_0 = 10^2$. It can be found that a high coupling efficiency close to 1 is achieved, when Q_b is arranged from 10^3 to 10^4 and k ($k = Q_\mathrm{b}/Q_\mathrm{d}$) is about 10 or even lower.

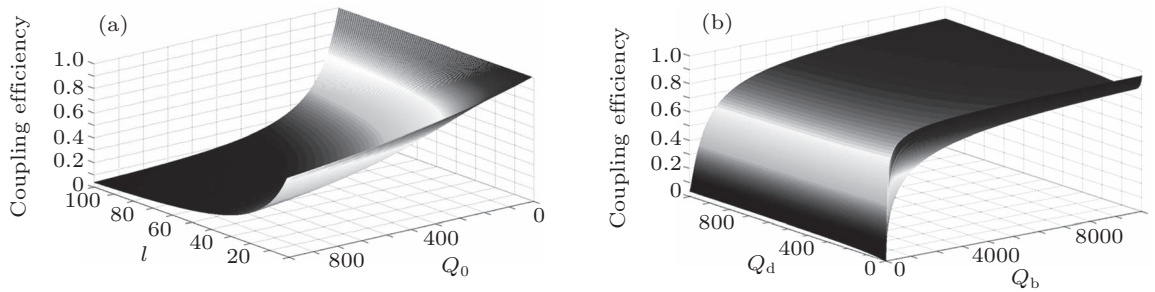

Fig. 3. (a) Coupling efficiency versus Q_0 and the total number of resonators. (b) Coupling efficiency as functions of Q_b and Q_d.

3. The side-coupled waveguide

On the basis of the structure illustrated in Section 2, we constructed an SCW with square array silicon rods in a silicon-on-insulator (SOI). The five-resonator array is placed on the side of the PC waveguide. A schematic of the SCW is shown in Fig. 4. The light is confined in the silicon rod by the photonic crystal band gap in the x–z plane and conventional total internal reflection in the vertical (y) direction. We consider a 2D PC composed of square array silicon rods in air with a lattice constant $p = 510$ nm. The rods are designed to be 400 nm in height. The radius and refractive index of the rods are $r = 0.2p$ and $n = 3.4$, respectively. The normalized frequency of the TM photonic band gap extends from 0.29 to 0.42, which is calculated using the plane wave expansion method.

As shown in Fig. 4(a), the SCW is composed of the side-coupling part that relies on five resonators and the waveguide part. Point defects consisting of rods with a radius ($r_\mathrm{p} = 0.1p$) smaller than that of the surroundings are introduced to construct the PC resonators. The resonance wavelength is 1550 nm. Since the coupling efficiency reaches the peak at $\beta d = 2n\pi$ ($n = 0, 1, 2, \ldots$), in view of the direct coupling, the interval of the resonators is set to be $6p$.[23] The waveguide part is composed of line defects consisting of rods with radius $r_l = 0.06$ μm. The structure parameters are shown in Fig. 4(b). By virtue of five resonators, the light wave is coupled into ports 1 and 2. Part of the light wave leaks out as the reflection loss. As shown in Fig. 4(c), a monitor is introduced to record the energy loss, and two monitors are also placed inside ports 1 and 2 to record the output energy. A TM light source with large scale is placed on the side of the SCW. In this paper, we focus on the condition where the light is projected on the resonator array along the z direction in the x–z plane. The coupling efficiency is sensitive to the incident angle. At normal incidence, light is coupled into the waveguide part through the resonator array efficiently. Otherwise, the output powers of the two ports will be different, and the coupling efficiency will decline slightly. Normal incidence is achieved when the output power reaches the maximum value and is equal to each other.

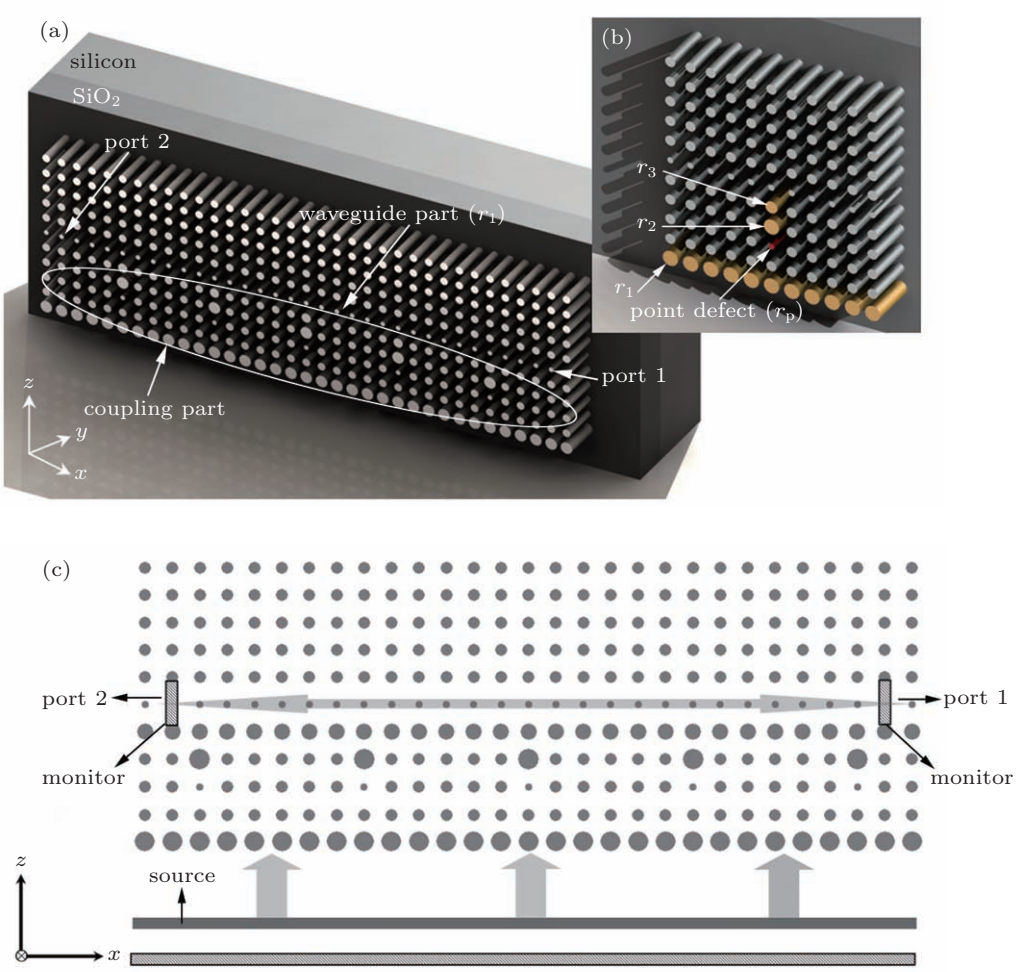

Fig. 4. (colour online) (a) A side coupling system composed of two parts: the coupling part and the waveguide part. The coupling part is composed of five resonators, and the waveguide part is composed of a line defect with rods of a radius smaller than that of the surroundings. (b) One resonator unit of an SCW. The radii of the rods located around the point defects (r_1, r_2 and r_3) are optimized. (c) The structure schematic of an SCW. Two monitors are placed in ports 1 and 2 to record the output power.

The coupling efficiency is defined as the value of the output power divided by the incident power, as shown in Eq. (5). In this paper we focus on the coupling between the PC waveguide and the resonator array, and the transmission loss is ignored. Therefore, the incident power is equal to the sum of the output power and the reflection loss, and the coupling efficiency can be written as

$$\eta = \frac{I_1 + I_2}{I_{\mathrm{i}}}, \tag{13}$$

where I_1 and I_2 are, respectively, the output powers of ports 1 and 2, and I_{i} is the input power.

The coupling efficiency of SCW is only about 40% before optimization. As discussed in Section 1, to enhance the coupling efficiency, the key point is to gain a high Q_{b} and increase k ($k = Q_{\mathrm{b}}/Q_{\mathrm{d}}$). The radius of the rods around the point defect will influence the values of Q_{b} and Q_{d} dramatically. The curves of Q_{b} and Q_{d} as functions of r_1 are shown in Fig. 5(a). At the point of $r_1 = 0.23$ μm, the value of Q_{b} reaches about 1.3×10^4, while Q_{d} is about 1800. The curves of Q_{b} and Q_{d} as functions of r_2 and r_3 are shown in Figs. 5(b) and 5(c), respectively. At the points of $r_1 = 0.23$ μm, $r_2 = 0.26$ μm, and $r_3 = 0.12$ μm, Q_{b} reaches about 1.7×10^4, while Q_{d} is about 90. The value of k reaches about 200. According to the theory analyzed in Section 2, the SCW can work efficiently when $Q_{\mathrm{b}} = 1.7 \times 10^4$ and $k = 200$.

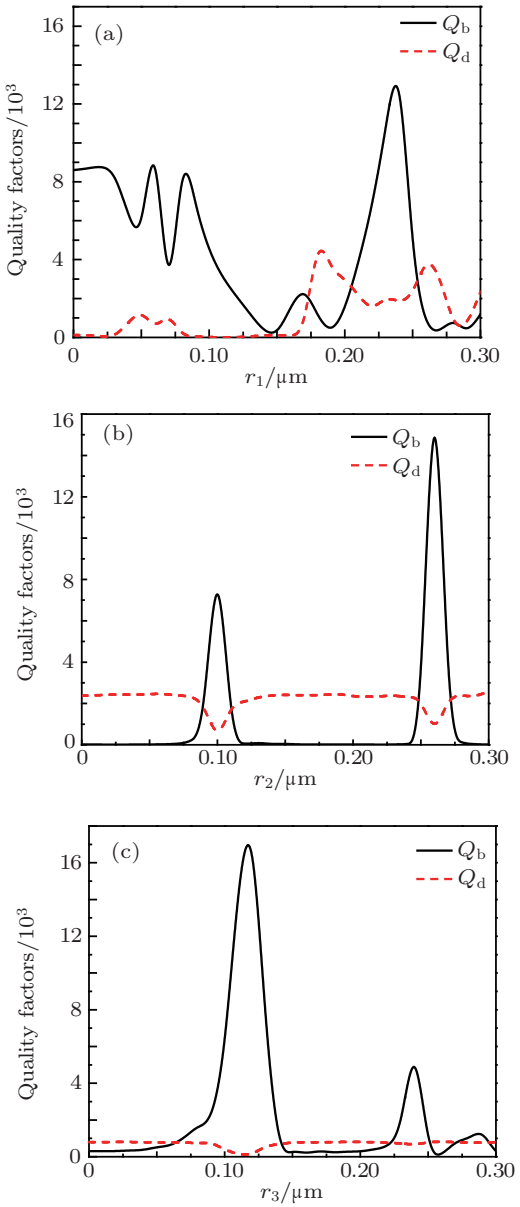

Fig. 5. (colour online) Optimization of the structure parameters. (a) The curves of Q_b and Q_d as functions of r_1. (b) The curves of Q_b and Q_d as functions of r_2. (c) The curves of Q_b and Q_d as functions of r_3.

Figure 6(a) shows the transmission spectrum of the SCW. At the selecting wavelength of 1550 nm, the monitor values of ports 1 and 2 reach the peaks, and the energy loss is nearly zero. Figure 6(b) shows the transmission characteristics of the SCW. The monitor values of ports 1 and 2 are both 6.8, owing to the symmetry of the SCW, and the reflection loss of the SCW is about 0.645. From Eq. (13), the total coupling efficiency of the two channels is calculated to be 95.47%. Figure 6(c) shows the field pattern of the system. The electromagnetic wave is concentrated in the waveguide part, while the energy loss is low by contrast. The simulation is performed using the finite difference time-domain method with the perfectly matched layer absorbing boundary condition.

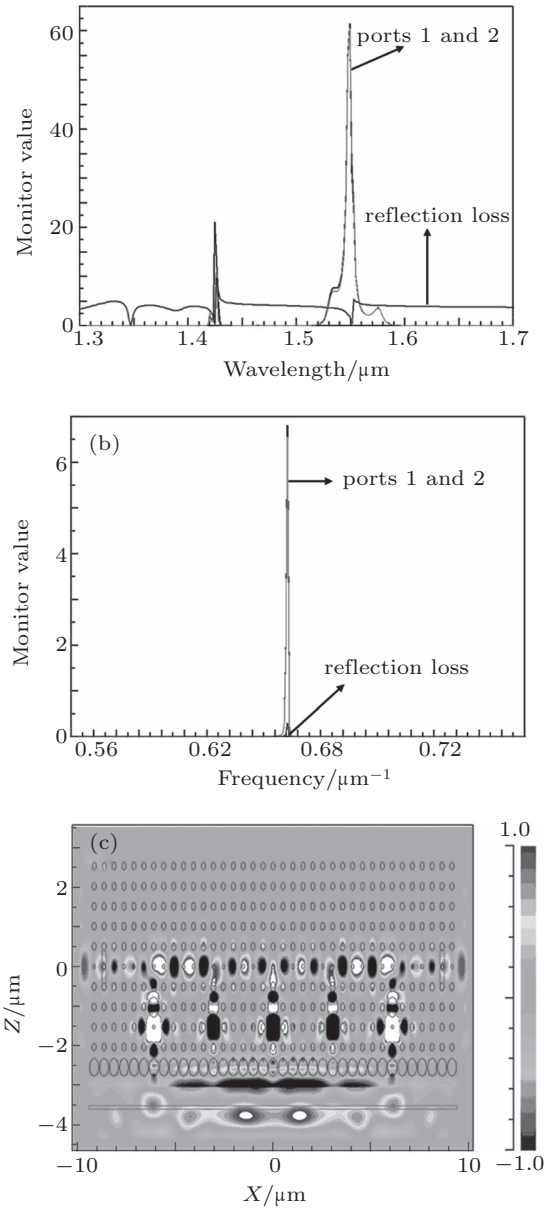

Fig. 6. The transmission characteristics of the SCW. (a) The transmission spectrum of the SCW. (b) The monitor values of the output power and the reflection loss. (c) The field pattern of the SCW when the Gaussian wave propagates at the resonant frequency.

Based on the above results, it is shown that the SCW couples with the lightwaves efficiently, the energy density in the waveguide is much higher, and the two channels of the SCW can also be utilized as T-type PC waveguides.

4. Conclusions

The coupling mode theory of a resonator array has been analyzed, which may be of significant value

for PC coupling devices. It is found that the coupling efficiency of the SCW can be influenced by the interval, the total number and the Q factors (Q_0, Q_b and Q_d) of the resonators. Based on the resonator array, the SCW is proposed to realize efficient coupling between the PC devices and the light source. Five parallel resonators with an interval of $6p$ are selected in view of the coupling efficiency and the coupling region. The intrinsic loss of resonators can be restrained by designed SCW in SOI due to the total internal reflection at the interface between the rods and the substrate/air clad. Q_b and Q_d are modulated through optimizing the radius of the rods located near the point defects of the resonators. When $r_1 = 0.23$ μm, $r_2 = 0.26$ μm and $r = 0.12$ μm, the theoretical coupling efficiency is 95.47%. Compared with the GOC and EWC methods, SCW shows the following advantages: a high integration level, a low degree of operational difficulty, a compact structure and near-unity coupling efficiency.

Acknowledgements

The authors are grateful to Dr. Dai Qi-Lin for his beneficial discussions, and Dr. Lü Jin-Guang and Dr. Feng Cong for their help during this work.

Appendix A

The complexity degree of A_n and the coupling efficiency η depends on the amount of resonators. The coupled mode theory of l resonators is analyzed using numerical calculation software. Herein, we give the expression when the coupling part is composed of five parallel resonators.

Resolving Eq. (9), we obtain

$$\begin{aligned}\sum\nolimits_1^l A_n = \frac{a}{Q_\mathrm{b}}[&(6\tau_\mathrm{b}\tau_\mathrm{d}r^4HQ_\mathrm{b} - 8\tau_\mathrm{b}\tau_\mathrm{d}r^3HQ_\mathrm{b}\\ &- 2\tau_\mathrm{b}\tau_\mathrm{d}r^2HQ_\mathrm{b} - 16\tau_\mathrm{b}\tau_\mathrm{d}rHQ_\mathrm{b}\\ &- 14\tau_\mathrm{b}\tau_\mathrm{d}r^4\omega_0 - 12\tau_\mathrm{b}\tau_\mathrm{d}r^3\omega_0 - 14\tau_\mathrm{b}\tau_\mathrm{d}r^2\omega_0\\ &+ 4\tau_\mathrm{d}^2r^4\omega_0 + 8\tau_\mathrm{d}^2r^3\omega_0 + 12\tau_\mathrm{d}^2r^2\omega_0\\ &+ 16\tau_\mathrm{d}^2r\omega_0 - 6\tau_\mathrm{b}^2r^4HQ_\mathrm{b} + 12\tau_\mathrm{b}^2r^3HQ_\mathrm{b}\\ &- \tau_\mathrm{b}^2r^2HQ_\mathrm{b} + 20\tau_\mathrm{d}^2HQ_\mathrm{b} + 10\tau_\mathrm{b}^2r^4\omega_0)\\ &\times (2\tau_\mathrm{b}^3r^4 - 4\tau_\mathrm{b}^2\tau_\mathrm{d}r^4 + 2\tau_\mathrm{b}\tau_\mathrm{d}^2r^4 - 3\tau_\mathrm{b}^2\tau_\mathrm{d}r^2\\ &+ 2\tau_\mathrm{b}\tau_\mathrm{d}^2r^2 + 4\tau_\mathrm{d}^3)^{-1}]^2, \end{aligned} \tag{A1}$$

where τ_b and τ_d are the coupling coefficients associated with the wave coupled into the bus waveguide and the wave decayed out of the resonator, respectively. They can be expressed as

$$\tau_\mathrm{b} = \mathrm{e}^{\mathrm{j}\theta_\mathrm{b}}\sqrt{\frac{\omega_0}{2Q_\mathrm{b}}}, \tag{A2}$$

$$\tau_\mathrm{d} = \mathrm{e}^{\mathrm{j}\theta_\mathrm{d}}\sqrt{\frac{\omega_0}{2Q_\mathrm{d}}}. \tag{A3}$$

The coupling efficiency η is expressed as

$$\begin{aligned}\eta = \frac{1}{4}[&(2\tau_\mathrm{d}HQ_\mathrm{b} - 11\tau_\mathrm{b}\tau_\mathrm{d}r^4\omega_0 - 2\tau_\mathrm{b}^2r^2HQ_\mathrm{b}\\ &+ 6\tau_\mathrm{d}^2\omega_0r^4 - 5\tau_\mathrm{b}\tau_\mathrm{d}r^3\omega_0 - 2\tau_\mathrm{b}\tau_\mathrm{d}r^2\omega_0\\ &- 6\tau_\mathrm{b}\tau_\mathrm{d}r^3HQ_\mathrm{b} + 3\tau_\mathrm{d}^2r^2\omega_0 + 4\tau_\mathrm{b}^2r^4\omega_0\\ &- 2\tau_\mathrm{b}\tau_\mathrm{d}rHQ_\mathrm{b} + \tau_\mathrm{d}^2r\omega_0 + 4\tau_\mathrm{d}^2\omega_0r^3 + 4s^2r^3HQ_\mathrm{b}\\ &- 7\tau_\mathrm{b}\tau_\mathrm{d}r^6\omega_0 - 7\tau_\mathrm{b}\tau_\mathrm{d}r^5\omega_0 - 8\tau_\mathrm{b}^4r^5Q_\mathrm{b}\\ &+ 2\tau_\mathrm{d}^2r^6\omega_0 - 8\tau_\mathrm{b}\tau_\mathrm{d}r^4HQ_\mathrm{b} + 8\tau_\mathrm{b}^2r^4HQ_\mathrm{b}\\ &+ 2\tau_\mathrm{d}^2rHQ_\mathrm{b} + 2\tau_\mathrm{d}^2r^4HQ_\mathrm{b} - 2\tau_\mathrm{b}\tau_\mathrm{d}^3Q_\mathrm{b}\\ &- 2\tau_\mathrm{b}\tau_\mathrm{d}^3r^3Q_\mathrm{b} - 2\tau_\mathrm{b}^2\tau_\mathrm{d}^2r^3Q_\mathrm{b} - 2\tau_\mathrm{b}^2\tau_\mathrm{d}^2r^7Q_\mathrm{b}\\ &+ 6\tau_\mathrm{b}^3\tau_\mathrm{d}r^3Q_\mathrm{b} - 4\tau_\mathrm{b}^2\tau_\mathrm{d}^2r^5Q_\mathrm{b} + 14\tau_\mathrm{b}^3\tau_\mathrm{d}r^5Q_\mathrm{b}\\ &- 4\tau_\mathrm{b}^2\tau_\mathrm{d}^2r^4Q_\mathrm{b} - 4\tau_\mathrm{b}\tau_\mathrm{d}r^2HQ_\mathrm{b} - 2\tau_\mathrm{b}\tau_\mathrm{d}^3r^2Q_\mathrm{b}\\ &- 8\tau_\mathrm{b}^4r^8Q_\mathrm{b} - 2\tau_\mathrm{b}^2\tau_\mathrm{d}^2r^8Q_\mathrm{b} - 4\tau_\mathrm{b}^2\tau_\mathrm{d}^2r^6Q_\mathrm{b}\\ &- 2\tau_\mathrm{b}\tau_\mathrm{d}^3rQ_\mathrm{b} + 8\tau_\mathrm{b}^3\tau_\mathrm{d}r^7Q_\mathrm{b} + 4\tau_\mathrm{b}^2r^7\omega_0\\ &+ 4\tau_\mathrm{b}^2r^7\omega_0 - 2\tau_\mathrm{b}^2\tau_\mathrm{d}^2r^2Q_\mathrm{b} - 8\tau_\mathrm{b}^4r^7Q_\mathrm{b} - 8\tau_\mathrm{b}^4r^4Q_\mathrm{b}\\ &+ 4\tau_\mathrm{b}^2r^6\omega_0 + 2\tau_\mathrm{b}^2r^3HQ_\mathrm{b} + 6\tau_\mathrm{b}^3\tau_\mathrm{d}r^2Q_\mathrm{b}\\ &+ 2\tau_\mathrm{d}^2r^2HQ_\mathrm{b} + 4\tau_\mathrm{b}^2r^8\omega_0 + \tau_\mathrm{d}^2r^8\omega_0 + \tau_\mathrm{d}^2r^7\omega_0\\ &+ 4\tau_\mathrm{b}^2r^5\omega_0 + 14\tau_\mathrm{b}^3\tau_\mathrm{d}r^4Q_\mathrm{b} - 8\tau_\mathrm{b}^4r^6Q_\mathrm{b}\\ &- 4\tau_\mathrm{b}\tau_\mathrm{d}r^8\omega_0 + 8\tau_\mathrm{b}^3\tau_\mathrm{d}r^8Q_\mathrm{b} - 4\tau_\mathrm{b}\tau_\mathrm{d}r^7\omega_0\\ &- 2\tau_\mathrm{b}\tau_\mathrm{d}^3r^4Q_\mathrm{b} + 14\tau_\mathrm{b}^3\tau_\mathrm{d}r^6Q_\mathrm{b})/(-4\tau_\mathrm{b}\tau_\mathrm{d}r^3HQ_\mathrm{b}\\ &+ 12\tau_\mathrm{b}^2r^3HQ_\mathrm{b} + 3\tau_\mathrm{b}\tau_\mathrm{d}r^4HQ_\mathrm{b}\\ &- 6\tau_\mathrm{b}^2r^4HQ_\mathrm{b} + 3\tau_\mathrm{d}^2r^2\omega_0\\ &- \tau_\mathrm{b}\tau_\mathrm{d}r^2HQ_\mathrm{b} - 7\tau_\mathrm{b}\tau_\mathrm{d}r^4\omega_0 - \tau_\mathrm{b}^2r^2HQ_\mathrm{b}\\ &+ 5\tau_\mathrm{d}^2HQ_\mathrm{b} + \tau_\mathrm{d}^2r^4\omega_0 - 6\tau_\mathrm{b}\tau_\mathrm{d}r^3\omega_0\\ &- 7\tau_\mathrm{b}\tau_\mathrm{d}r^2\omega_0 + 2\tau_\mathrm{d}^2r^3\omega_0 + 10\tau_\mathrm{b}^2r^4\omega_0\\ &- 8\tau_\mathrm{b}\tau_\mathrm{d}r^HQ_\mathrm{b} + 4\tau_\mathrm{d}^2r_0^\omega)^{-1}]^2. \end{aligned} \tag{A4}$$

References

[1] Yablonovitch E 1987 *Phys. Rev. Lett.* **58** 2059
[2] John S 1987 *Phys. Rev. lett.* **58** 2486
[3] Joannopoulos J D, Villeneuve P R and Fan S 1997 *Nature* **386** 143
[4] Sugisaka J, Yamamoto N, Okano M, Komori K, Yatagai T and Itoh M 2008 *Opt. Commun.* **281** 5788
[5] Lu H, Tian H P, Li C H and Ji Y F 2009 *Acta Phys. Sin.* **58** 2049 (in Chinese)
[6] Zhang X, Tian H P and Ji Y F 2010 *Opt. Commun.* **283** 1768

[7] Tada T, Poborchii V V and Kanayama T 2002 *Micro. Eng.* **63** 259

[8] Liu L Y, Tian H P and Ji Y F 2011 *Acta Phys. Sin.* **60** 104216 (in Chinese)

[9] Hu X Y, Jiang P, Ding C Y, Yang H and Gong Q H 2008 *Nat. Photonics* **2** 185

[10] Hitoshi N, Suginoto Y, Kanamoto K, Ikeda N, Tanaka Y, Nakamura Y, Ohkouchi S, Watanabe Y, Inoue K, Ishikawa H and Asakawa K 2004 *Opt. Express* **12** 6606

[11] Liu C Y 2009 *Phys. Lett.* A **373** 3061

[12] Sharkawy A, Shi S and Prather D W 2001 *Appl. Opt.* **40** 2247

[13] Faraon A, Waks E, Englund D, Fushman I and Vučković J 2007 *Appl. Phys. Lett.* **90** 073102

[14] Tong X, Han K, Shen X P, Wu Q H, Zhou F, Ge Y and Hu X J 2011 *Acta Phys. Sin.* **60** 064217 (in Chinese)

[15] Yang W, Chen X S, Shi X Y and Lu W 2010 *Physica* B **405** 1832

[16] Matsumoto T, Fujita S and Baba T 2005 *Opt. Express* **13** 10768

[17] Takano H, Akahane Y, Asano T and Noda S 2004 *Appl. Phys. Lett.* **84** 2226

[18] Fukaya N, Ohsaki D and Baba T 2000 *Jpn. J. Appl. Phys.* **39** 2619

[19] Lin C Y, Wang X L, Chakravarty S, Lee B S, Lai W C and Chen R T 2010 *Appl. Phys. Lett.* **97** 183302

[20] Barclay P E, Srinivasan K, Borselli M and Painter O 2004 *Opt. Lett.* **29** 697

[21] Martijn de Sterke C, Dossou K B, White T P, Botten L C and McPhedran R C 2009 *Opt. Express* **17** 17338

[22] Xu Y, Li Y, Lee R K and Yariv A 2000 *Phys. Rev.* E **62** 7389

[23] Ren H L, Jiang C, Hu W S, Gao M Y and Wang J Y 2006 *Opt. Express* **14** 2446

[24] Zhang Z Y and Qiu M 2005 *Opt. Express* **13** 2596

[25] Manolatou C, Khan M J, Fan S H, Villeneuve P R and Hans H A 1999 *IEEE J. Quantum Electron.* **35** 1322

[26] Nanaee M G and Young J F 2008 *Opt. Express* **16** 20908

[27] Akahane Y, Asano T, Song B S and Noda S 2003 *Nature* **425** 944

[28] Faraon A, Waks E, Englund D, Fushman I and Vuckovic J 2007 *Appl. Phys. Lett.* **90** 073102

[29] Tada T, Poborchii V V and Kanayama T 2002 *Microelectron Eng.* **63** 259

[30] Poborchii V V, Tada T and Kanayama T 2002 *J. Appl. Opt.* **91** 3299